Formation mechanism and energy levels of GaN six-bilayer periodic structures grown on GaAs(001)

Mitsuru Funato,* Shizuo Fujita, and Shigeo Fujita

Department of Electronic Science and Engineering, Kyoto University, Kyoto 606-8501, Japan

(Received 22 March 2000; revised manuscript received 19 July 2000; published 4 April 2001)

The formation mechanism and energy levels of six-bilayer periodic structures in GaN on GaAs(001), which we found recently [Appl. Phys. Lett. **76**, 330 (2000)], are investigated. Transmission electron microscopy suggests that the periodicity originates at valleys formed by zinc-blende (ZB) and wurtzite (W) phases, and develops along the ZB-$\langle 111 \rangle A$ direction. On the basis of this observation, we propose that the competition between ZB and W phases during the growth is a driving force for the formation of the periodic structures. From the six-bilayer periodic structures, photoluminescence is observed at 20 K, and its peak position agrees well with a calculation based on the Kronig-Penney model, in which the periodic structures are regarded as ZB/W superlattices.

I. INTRODUCTION

The most stable crystalline structure of GaN is wurtzite (W), and optoelectronic devices now available commercially have been fabricated with W-GaN.[1–3] Zinc-blende (ZB) structure can also be grown epitaxially by selecting proper substrates, such as GaAs(001), and growth conditions.[4–7] However, the ZB structure is metastable, which makes it energetically favorable to introduce stacking faults in ZB films because ZB faults on the basal planes inevitably contain the lower-energy W stacking. We showed in a preceding paper that, as a result of the inclusion of basal-plane stacking faults into ZB films, six-bilayer periodic structures as well as W phases appeared in GaN grown on GaAs(001).[8] Possible stacking sequences were proposed to be $ABCBAC$ or $ABCBAB$ (or its twin, that is, $ABABAC$), which are classified as 6H polytypes. (In this notation, each letter stands for an ordered pair of cation and anion layers.) It is interesting to assess the stability of GaN polytypes quantitatively. Using an approach employed previously by Cheng *et al.*[9] to study polymorphism in SiC, and using the interaction energies between GaN molecular layers calculated by Wright,[10] we evaluated the total energies for ZB (. . . $ABCABC$ . . .), $ABCBAC$, and $ABCBAB$, with respect to W (. . . $ABABAB$ . . .), to be 11.7, 7.3, and 3.5 meV per cation-anion pair, respectively. A positive sign means an increase in the energy; therefore, six-bilayer periodic structures are more stable than the ZB structure, implying that single-phase six-bilayer structures may be obtained more easily than a single-phase ZB structure.

In this study, the formation mechanism of six-bilayer periodic structures in GaN grown on GaAs(001) is investigated chiefly by high-resolution (HR) transmission electron microscopy (TEM). Furthermore, in order to gain some insight into the properties of these interesting structures, photoluminescence (PL) measurements are performed at 20 K, and the observed peak position is compared with a calculation based on the Kronig-Penney model, in which the periodic structures are regarded as ZB/W superlattices.

II. EXPERIMENT

GaN thin films were grown on GaAs(001) substrates by atmospheric-pressure metal-organic vapor-phase epitaxy (MOVPE). The GaAs substrates were cleaned chemically and thermally in the conventional manner. The gallium and the nitrogen sources were triethylgallium and dimethylhydrazine, respectively. A 20-nm-thick GaN buffer layer was grown on GaAs at 600 °C under a V/III ratio of 100. Then a GaN layer was grown at higher temperatures of 800–920 °C with V/III ratios of 25–50. For the formation of the six-bilayer periodic structure, it is important to promote the inclusion of basal-plane stacking faults into ZB-GaN. Therefore, the growth condition was not optimized in terms of the ZB composition, and grown GaN was made up of a mixture of a ZB phase, a W phase with W-[0001] ∥ ZB-$\langle 111 \rangle A$, and six-bilayer periodic structures.[11] The compositions of the three phases were basically in the order ZB>W> six-bilayer periodic structure.

For TEM observations, samples were prepared by conventional Ar$^+$ milling. We have already shown that six-bilayer periodicity occurs along the ZB-$\langle 111 \rangle A$ direction,[8] and therefore $(\bar{1}10)$ cross sections, which inform us about $\{111\}A$ layer stacking, were observed. PL measurements were conducted at 20 K with a He-Cd laser (325 nm) as an excitation source. PL was detected using a cooled charge-coupled device in conjunction with a 50-cm monochromator. The spectral resolution was as small as 0.2 nm. This value corresponded to ∼2 meV in the energy region which includes the GaN band-gap energy.

III. FORMATION MECHANISM

Figure 1 shows (a) an electron diffraction (ED) pattern and (b) a large area TEM dark-field image of the $(\bar{1}10)$ cross section. In the ED pattern, in addition to the diffraction spots from GaAs, ZB-GaN, and W-GaN, extra spots aligned along ZB-$\langle 111 \rangle A$ are observable, one of which is indicated by the arrowhead. These extra spots originate from the six-bilayer periodic structures, as will be proved below. Since the minimum-size objective aperture of the TEM system still
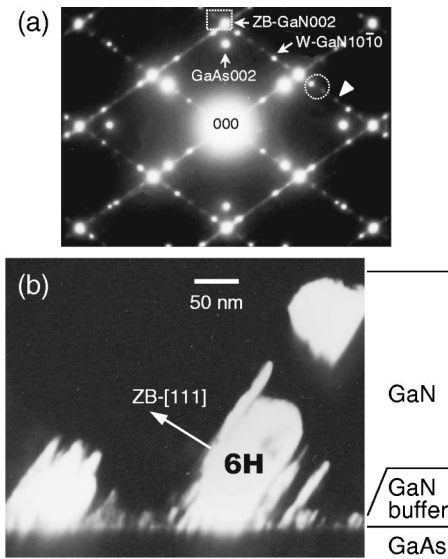
FIG. 1. (a) ED pattern and (b) TEM dark-field image of GaN grown on GaAs(001). The ($\bar{1}10$) cross section was observed. The arrowhead in (a) shows one of the diffraction spots from six-bilayer periodic structures. Also in (a), the circle indicates the size of the objective aperture, inside which are the diffraction spots used to generate the dark-field image of (b). The rectangle in (a) is used with Fig. 3.
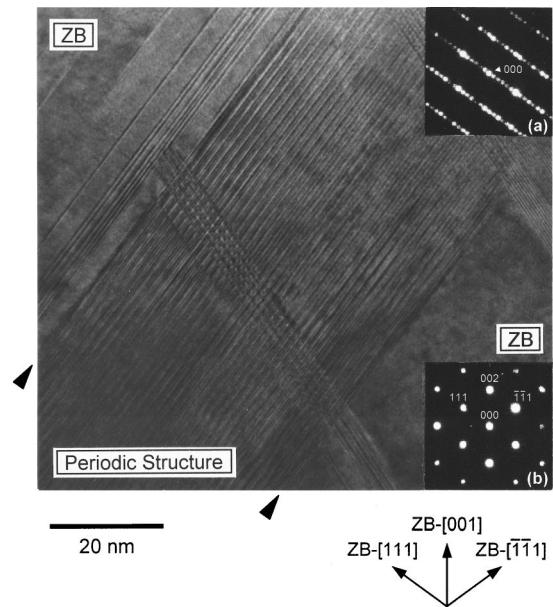

FIG. 2. HR image of the six-bilayer periodic structure. The arrowheads indicate the boundaries between the six-bilayer periodic structure and the ZB phases. The insets are the ED patterns from (a) the periodic structure and (b) the pure ZB phase.

includes two diffraction spots, the dark-field image of Fig. 1(b) was generated from an extra diffraction spot and the neighboring W-GaN10$\bar{1}\bar{1}$ diffraction spot, which are surrounded by the circle in the ED pattern. Therefore, the bright contrast in the dark-field image is either a six-bilayer periodic structure or W phase. It should be noted that the W diffraction spot always overlaps with the diffraction spot from the six-bilayer periodic structures (6H), because wurtzite belongs to the hexagonal structure. Therefore, more strictly, two diffraction spots from six-bilayer periodic structures are included in the objective aperture (one of them overlaps with W-GaN10$\bar{1}\bar{1}$), and interference fringes should be observed in the region where six-bilayer periodicity occurs. By observing the interference fringes, the domain designated by 6H was confirmed to possess a six-bilayer periodicity along the ZB-[111] direction, while other domains were in the W phase. The dimensions of the six-bilayer structure were estimated to be 80 nm in the ZB-[111] direction and 150 nm in the direction perpendicular to ZB-[111]. This is the largest domain we have detected, and the dimensions appeared to differ considerably from domain to domain. In this sample, the roughly estimated fractional occupancy of the six-bilayer periodic structures was in the range of 5–10 %, and that of the W phase was a few tens of percent.

In order to see the structural properties of the film in more detail, HRTEM images and microbeam (1 nm in diameter) ED patterns were taken. Regarding the W phase, it was often observed that W domains, such as those observed in Fig. 1, contain few stacking faults. The largest W-GaN domain without a stacking fault was approximately 50 nm thick along the c axis ($\parallel$ ZB-$\langle 111 \rangle A$). The reason why such a

large domain of nearly pure W phase can be grown even on the ZB-GaAs(001) substrate is not well understood. A basal-plane stacking fault in the ZB phase due to the lattice mismatch between GaN and GaAs may have initiated the W domain, because this induces W stacking and provides a W-(0001) template. Regarding the six-bilayer periodic structure, on the other hand, the observed results are shown in Fig. 2. As is seen in the HRTEM image, six-bilayer periodicity (15.6 Å) occurs along the ZB-[111] direction. In this particular case, the periodic structure is sandwiched by ZB phases along the ZB-[111] direction. A comparison between ED patterns from the periodic structure and from the ZB phase also verifies the six-bilayer periodicity along the ZB-[111] direction; in the ED pattern from the periodic structure, diffraction spots are aligned in the ZB-[111] direction, and the distance between the neighboring spots is exactly one-sixth that between the 000 and ZB-GaN111 diffraction spots.

It should be pointed out that a superposition of ZB and W phases within the specimen thickness can produce the same effects in cross-sectional images (moiré fringe). In order to eliminate this possibility, an x-ray reciprocal-space mapping (RSM) of the reciprocal ($\bar{1}10$) plane was conducted using Cu $K\alpha_1$ radiation as an x-ray source. The x-ray spot size was limited by a slit to be 0.2×2 mm^2, which is much larger than the dimensions of the six-bilayer periodic structures and the W phase (see Fig. 1). Therefore, information from all three phases is measured simultaneously. The measured area in reciprocal space is indicated by the rectangle in Fig. 1(a), where intensities from both ZB-GaN002 and the six-bilayer periodic structures should be detected. Figure 3 illustrates the measured reciprocal-space map. Indeed, two diffraction spots were observed; since diffraction spots due to the W phase and/or the twinned ZB phase do not appear in this area, we simply attribute one spot to ZB-GaN and the other to the
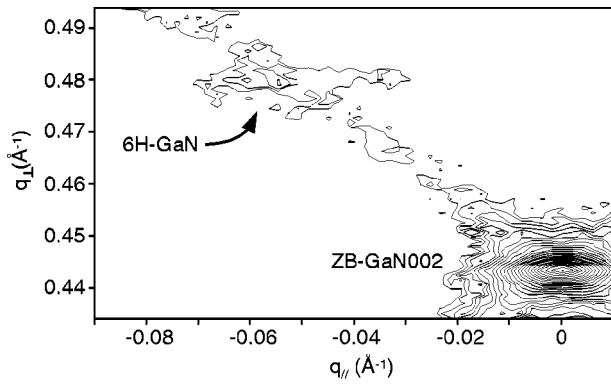
FIG. 3. The x-ray RSM of the area indicated by the rectangle in Fig. 3(a). Isointensity contour levels at $2^{n/3}$ ($n=0,1,2,3,\dots$) cps. The $q_{\parallel}$ axis is parallel to the [110] direction, and the $q_{\perp}$ axis is parallel to the [001] direction.

six-bilayer period structure. The position of the diffraction spot from the six-bilayer period structure is the same as that seen in ED patterns. If the superposition mentioned above had caused the extra spots in the ED patterns, those spots must disappear in x-ray RSM because the incident direction of the x rays is almost perpendicular to the electron-beam direction. The results of TEM and x-ray RSM are therefore complementary, and prove the presence of six-bilayer periodic structures.

Now a question arises as to how the six-bilayer periodic structures originate. In order to answer this question, the area where the periodic structure is generated was observed by HRTEM, and a typical example is shown in Fig. 4. In the figure, the bottom left is a ZB phase, and the right-hand side is a W phase whose c axis is parallel to the ZB-[111] direction. The periodic structure is located in between. This figure suggests that the atom growing on the ZB phase experiences a "force to be W," and compromises by forming a six-bilayer periodic structure.
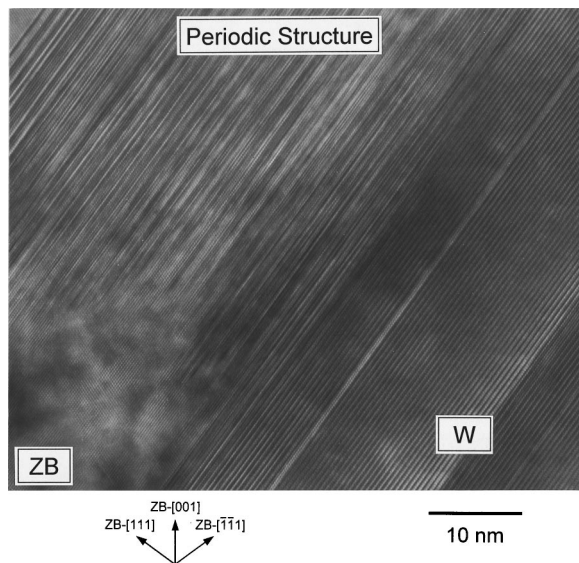

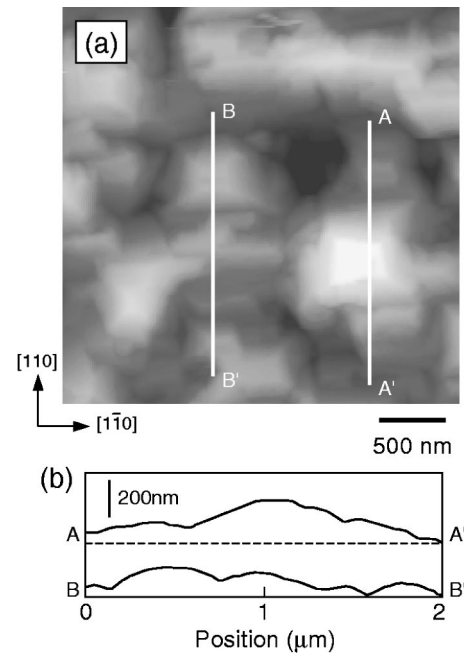FIG. 4. HR image showing a typical example of the area at which the periodic structure is generated.

FIG. 5. Surface structures of GaN including the six-bilayer periodic structures: (a) AFM image and (b) height profiles measured along AA' and BB' in (a).

The origin of this "force to be W" is still controversial, but will be related to the formation of the large W domain. (The presence of the large W domain was already discussed, and an example can also be seen on the right-hand side of Fig. 4.) Of course, the W phase on the right-hand side provides a W-(0001) template, on which GaN generally tends to grow in the stable W phase. Furthermore, the atomically rough surface of the ZB phase, which is implied by the rough interface between the ZB phase and the six-bilayer periodic structure (Fig. 4), can be a driving force for W-GaN growth because the atomic steps consist of ZB-{111}, which is equivalent to W-{0002}. To support this assertion experimentally, we confirmed by x-ray pole figure measurements that GaN grown on GaAs(001) misoriented toward $\langle 110 \rangle$ by 10° is predominantly made up of the W phase.[12] In addition to these, the influence of growth conditions should be considered. The present growth condition was not optimized for ZB-GaN, which can promote the growth of W-GaN.

Before discussing the formation mechanism of six-bilayer periodic structures, we show the surface structure of a grown sample, which will turn out to be important for generating the six-bilayer periodic structures. Figure 5(a) is a surface atomic force microscopy (AFM) image, while Fig. 5(b) shows height profiles measured along AA' and BB' in Fig. 5(a). An important finding from the AFM observation is that the surface does not always consist of singular planes such as {001} and {111}, as deduced from the height profiles. This indicates that a number of atomic steps exist on the surface. Comparison between the AFM (Fig. 5) and TEM [Fig. 1(b)] images provides further information on the surface atomic steps; judging from the dimensions of the three phases, the phase mixture does not correlate directly with large surface undulations of the order of a few hundred nanometers, but
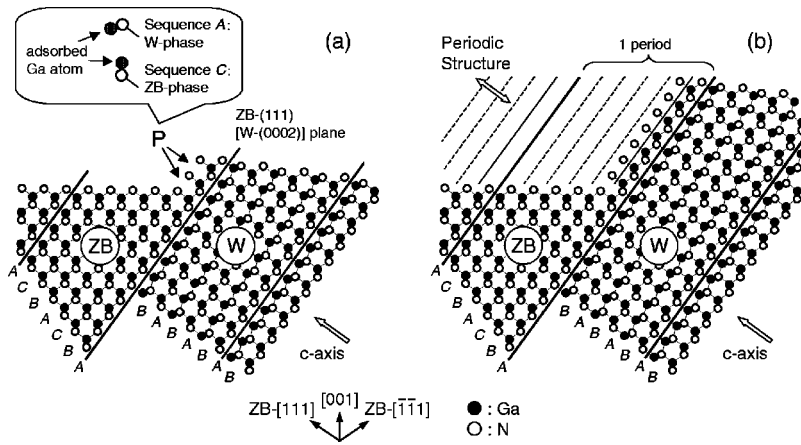
FIG. 6. A model for the formation mechanism of the six-bilayer periodic structure, (a) before and (b) after the formation. The inset in (a) shows the possible sequences for a Ga atom adsorbed at position P.

may cause small undulations which are more clearly seen in the height profiles [Fig. 5(b)]. This is quite natural, because the growth rates of the phases are not necessarily equivalent and, consequently, atomic steps are formed at phase boundaries. The same conclusion was extracted from cross-sectional HRTEM. Furthermore, it was confirmed by cross-sectional HRTEM that atomic steps showed various morphologies, that is, they exist not only at phase boundaries but also, for example, on pure ZB or W phases and at ZB/ stacking-fault interfaces.

Figures 4 and 5 provide interesting evidence for elucidating the formation mechanism of a periodic structure. The details are explained using a structure model illustrated in Fig. 6. Figure 6(a) shows the $(\bar{1}10)$ cross section before the formation of a periodic structure. Although atomic steps certainly exist on the ZB-(001) surface as well, here we simply drew the ZB surface by a flat (001) plane. As in the HR image of Fig. 4, the c axis of the W phase is in the ZB-[111] direction. Since ZB-(111) planes are equivalent to W-(0002) planes, the ZB and W phases are adjacent to each other via a stacking fault on a ZB-(111) [W-(0002)] plane. The existence of surface atomic steps like that illustrated in Fig. 6(a) was already described in connection with Fig. 5. Taking Fig. 5(b) into account, there will be many step structures like Fig. 6(a) on the surface.

Let us suppose that, under this atomic configuration, growth occurs at the step edge. This assumption is quite reasonable because step edges generally act as a major sink for migrating adatoms. Since MOVPE growth was performed under the nitrogen-excess condition in this study, here we consider only Ga atoms, which determine the growth characteristics. Figure 6(a) illustrates the situation in which a migrating Ga adatom reaches the step edge, position P. This Ga atom is influenced by both the ZB and W phases; the Ga atom can occupy either the ZB site or the W site, that is, the Ga site in sequence C or that in sequence A, as shown in the inset of Fig. 6(a). As the growth proceeds laterally along the ZB-(001) plane from position P, a similar situation might occur for the following several adatoms. This is because the layer stacking sequences for ZB and W are $ABCABC$ and $ABABAB$, respectively, and are different from each other in the latter four sequences ($CABC$ for the ZB phase and $ABAB$ for the W phase). Consequently, the

crystalline structure at the corresponding molecular layers becomes uncertain, and is determined by a compromise between the ZB and W phases. These layers are denoted by the dotted lines in Fig. 6(b).

On the other hand, the layer stacking sequences of ZB and W agree completely every six molecular layers, as is deduced from the sequences of ZB ($\ldots ABCABCA \ldots$) and W ($\ldots ABABABA \ldots$). Therefore, every sixth molecular layer definitely has an A stacking sequence even at the valley formed by the ZB and W phases, which is illustrated by the thick solid lines in Fig. 6. We believe this is the reason for the six-bilayer periodicity. Now the role of the atomic step at the surface before the formation of the periodic structures [Fig. 6(a)] is clear. The atomic step provides a template and a motive for forming six-bilayer periodic structures.

One may consider that the influence from the W phase at the right-hand side will fade away as the growth proceeds, and that a narrow region of the six-bilayer periodic structure results. However, as already described, we observed a nearly pure W-GaN with a dimension of a few tens of nanometers along the c axis. This result strongly suggests that the influence of the W phase can persist over a relatively long distance, and validates the present model for the formation mechanism of the six-bilayer periodic structure. It is worth noting that TEM observations were performed many times, and that the proposed mechanism was confirmed to be applicable to most of 6H domains.

The model shown here is an example of the origin. The essence is competition between the ZB and W phases, and a motive such as the atomic step shown in Fig. 6(a). In this sense, the following examples will also cause periodic structures: (1) a step structure consisting of a ZB-$(\bar{1}\bar{1}\bar{1})$ plane and a $(10\bar{1}1)$ plane of a W phase whose c axis is in the ZB-[111] direction (an inverted mesalike structure), and growth conditions favorable for ZB-GaN; (2) a step structure consisting of ZB-(001) and ZB-(111) planes, and growth conditions favorable for W-GaN; and (3) a step structure consisting of W-$(10\bar{1}1)$ and W-(0002) planes, and growth conditions favorable for ZB-GaN. In a future study, structured substrates will be a key to improving the fractional occupancy of the six-bilayer periodic structures.
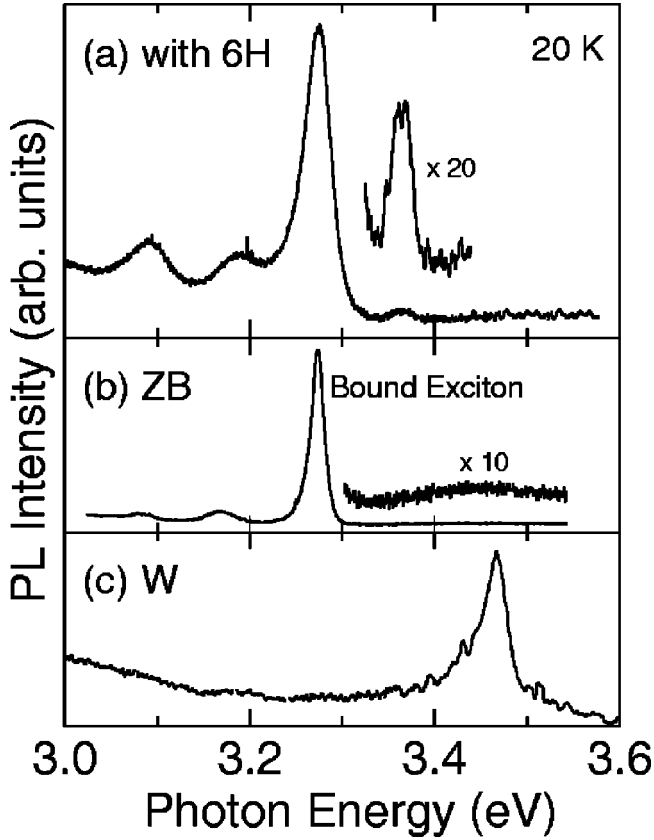
FIG. 7. (a) PL spectrum of GaN including six-bilayer periodic structures measured at 20 K. For comparison, PL spectra of (b) ZB-GaN with a higher ZB composition and (c) W-GaN grown in the same growth system are also shown.

TABLE I. Physical parameters used for the calculation. ΔE_c and ΔE_v denote the band discontinuities at the conduction and the valence bands, respectively, in units of eV. For W, the indicated effective masses are those along the c axis. Also, the hole effective mass is that at the A valence band.

| | Energy gap at 20 K (eV) | Effective mass | | ΔE_c | ΔE_v |
		electron	hole		
ZB	3.302 [a]	0.17 [b]	0.85 [b]	0.261	0.058
W	3.505 [c]	0.20 [b]	1.3 [d]		

[a]Reference 14.
[b]Reference 15.
[c]Estimated from Ref. 16.
[d]Reference 17.

IV. ENERGY LEVELS

Our next discussion concerns energy levels in the six-bilayer periodic structures. Figure 7(a) depicts a PL spectrum of GaN including six-bilayer periodic structures, measured at 20 K. The presence of the six-bilayer periodicity was confirmed by x-ray RSM, as in Fig. 3. For an assignment of origins of the observed four emissions, PL spectra of ZB-GaN with a higher ZB composition ($\sim$95%) and W-GaN grown in the same growth system are shown in Figs. 7(b) and 7(c), respectively. Comparing Figs. 7(a) and 7(b), it is found that the most intense emission in Fig. 7(a), peaking at 3.274 eV, originates from bound excitons in the ZB phase, which is the dominant phase in this sample. The peaks located below 3.2 eV are also from the ZB phase. No emission from the W phase, which would appear at around 3.47 eV as shown in Fig. 7(c), was observed. This will be discussed below. On the other hand, the weak emission at 3.364 eV, with a full width at half maximum (FWHM) of 25 meV, does not appear in the ZB- and W-GaN PL spectra, and characterizes the PL spectrum of GaN with six-bilayer periodic structures. Therefore, it is reasonable to consider that this peak is derived from six-bilayer periodic structures.

In x-ray RSM of GaN including six-bilayer periodic structures, the W diffraction was stronger than the diffraction due to the six-bilayer periodic structures, implying a larger composition of the W phase. However, excitonic emission from

the W phase was not observed in Fig. 7(a). The reason for this is unclear at present, but here we will point out two possibilities. One possibility is electron transfer from W-GaN to either ZB-GaN or to the six-bilayer structures, which weakens the emission from W-GaN. This is likely to occur because the conduction-band energy of W-GaN is the highest among the three phases. (For details, see the discussion with the Kronig-Penney model below.) The other possibility is the poor optical properties of W-GaN; if the quality of the W-GaN coexisting with ZB-GaN and the six-bilayer structure on GaAs(001) is not high, only yellow-band luminescence may be observed. In fact, the sample including six-bilayer periodic structures emitted deep-level luminescence. Although it was impossible to identify the phase responsible for this deep-level emission due to the broad emission width, further investigation of the relationship between the phase mixture and the optical properties using, for example, samples with different compositions will provide more conclusive evidence.

In order to support the assertion that the PL emission at 3.364 eV originates from six-bilayer periodic structures, a theoretical calculation was performed. Basically, hexagonal polytypes can be regarded as a structure where ZB and W phases are deposited with a certain order, that is, a ZB/W superlattice. For example, the $ABCBAB$ polytype can be considered to be a superlattice having a (W-ZB-W-ZB-W-W) stacking sequence as one period. To the calculation of energy levels in such superlattices, the Kronig-Penney model was applied.[13] The physical parameters used are listed in Table I. An explanation is required for the band discontinuities at the ZB/W interface. Since the band discontinuities have not been determined experimentally, we must use the results of a theoretical study. Murayama and Nakayama calculated the band structures of various semiconductors in W and ZB phases, using the first-principles pseudopotential method.[18] They showed that, regardless of material, the energy gap of W was located at a higher energy than that of ZB, that is, ZB/W heterojunctions possessed type-II band alignments. In particular, for the GaN ZB/W heterojunction, the band discontinuities at the conduction and the valence bands were evaluated to be 0.154 and 0.034 eV, respectively. However, as pointed out in Ref. 18, those quantities include serious errors due to the approximation made in the calcula-
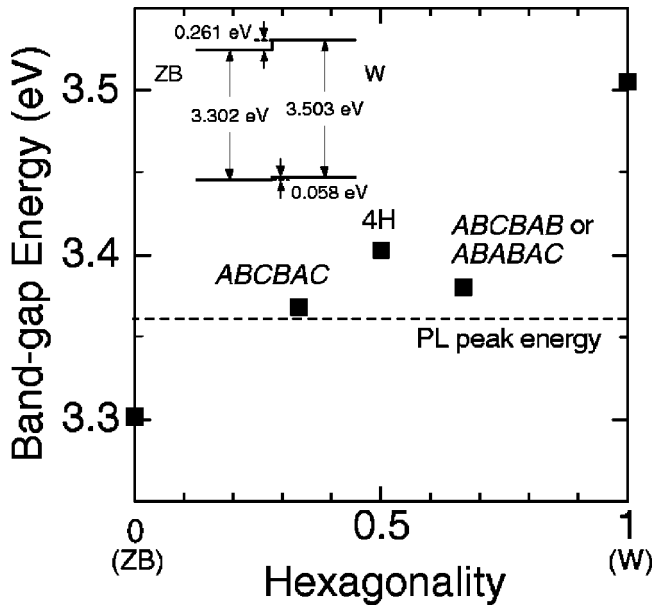
FIG. 8. Dependence of band-gap energies of several polytypes on hexagonality calculated by the simple Kronig-Penney model. The hexagonality refers to the proportion of W stacking. The dotted line indicates the PL peak position.

tion; generally, the difference between conduction- and valence-band discontinuities must be equal to the difference between W and ZB band-gap energies, but it is not (0.154 eV−0.034 eV=0.120 eV vs 3.505 eV −3.302 eV=0.203 eV). Therefore, in this study, the band discontinuities were deduced from the ratio of the theoretically calculated band discontinuities (0.154/0.034) and the actual difference of the band-gap energies (0.203 eV). Table I shows the discontinuities thus obtained.

Figure 8 shows the results of the Kronig-Penney calculations. The band-gap energy of the 4H polytype ($ABCB$) was also calculated for comparison. ''Hexagonality'' at the horizontal axis refers to the proportion of W stacking, and consequently, a hexagonality equal to 0 means a ZB configuration, while a hexagonality equal to 1 means a W configuration. As seen in the figure, the proposed stacking sequences have similar band-gap energies; 3.369 eV for the $ABCBAC$ sequence and 3.381 eV for the $ABCBAB$ or $ABABAC$ sequence. The 4H polytype has a larger band-gap energy of 3.403 eV. On the other hand, in the PL spectrum shown in Fig. 7(a), a peak was detected at 3.364 eV. This energy, which is designated by the dotted line in Fig. 8, agrees reasonably well with the calculations for six-bilayer periodic structures, supporting the hypothesis that the emission at 3.364 eV is derived from six-bilayer periodic structures. As pointed out in Ref. 8, the $ABCBAC$ and $ABCBAB$ sequences can coexist. The relatively broad FWHM of the

emission at 3.364 eV ($\sim$25 meV) implies the overlap of emissions from both sequences, though definite peak separation was not observed. Since PL is usually related to excitons at low temperatures, the emission energy is lowered, at least, by the exciton binding energy. Therefore, the observed difference between the PL peak energy and the calculated band-gap energies of 5–17 meV must be attributed chiefly to excitonic effects. Although this difference does not completely agree with the exciton binding energy of the A exciton in W-GaN ($\sim$28 meV),[16] this is probably due to an uncertainty in the physical parameters (the band discontinuities, in particular) used in the calculation and the inaccuracy of the calculation method. Another factor that may influence the emission energy is strain. However, strain is negligible in the present samples, because the monomolecular spacing estimated by x-ray RSM was 2.591 Å , which is almost the same as that in bulk GaN, 2.593 Å .[19,20]

Finally, we estimate how the uncertainty of the band discontinuities affects the present calculations. For this, the same calculation was performed with varying band discontinuities, while keeping a type-II band lineup. As a result, it was found that a $\pm$0.058-eV variation led to variation of only a few meV in the band-gap energies for $ABCBAC$ and 4H. For $ABCBAB$ (or $ABABAC$), the band-gap energies were calculated to be 3.353 eV, assuming a conduction-band discontinuity of 0.261+0.058 eV, and 3.398 eV for that of 0.261−0.058 eV. Although this variation is larger than that for $ABCBAC$, these values are still close to the observed PL emission energy of 3.364 eV. These results confirm that the model used in this study is rather simple, though very applicable to the explanation of the PL properties.

V. CONCLUSIONS

The formation mechanism and the PL properties of the six-bilayer periodic structures (6H polytypes) in GaN grown on GaAs(001) by MOVPE were studied. The periodic structures were found to be initiated at the valley between ZB and W phases. From this observation, we proposed that a competition between ZB and W phases during the growth is responsible for determining the layer stacking sequence. In the PL spectrum taken at 20 K, an emission peak was detected at 3.364 eV. Comparing with the Kronig-Penney calculation, this emission was attributed to six-bilayer periodic structures.

ACKNOWLEDGMENTS

---

*Electronic mail: funato@kuee.kyoto-u.ac.jp

[1] S. Nakamura, M. Senoh, N. Iwasa, S. Nagahama, T. Yamada, and T. Mukai, Jpn. J. Appl. Phys. **34**, L1332 (1995).

[2] S. Nakamura, M. Senoh, S. Nagahama, N. Iwasa, T. Yamada, T. Matsushita, H. Kiyoku, Y. Sugimoto, T. Kozaki, H. Umemoto,

M. Sano, and K. Chocho, Appl. Phys. Lett. **72**, 2014 (1998).

[3] S. Nakamura, M. Senoh, S. Nagahama, T. Matsushita, H. Kiyoku, Y. Sugimoto, T. Kozaki, H. Umemoto, M. Sano, and T. Mukai, Jpn. J. Appl. Phys. **38**, L226 (1999).

[4] D. Schikora, M. Hankeln, D. J. As, K. Lischka, T. Litz, A. Waag,

T. Buhrow, and F. Henneberger, Phys. Rev. B **54**, R8381 (1996).

[5] H. Tachibana, T. Ishido, M. Ogawa, M. Funato, Sz. Fujita, and Sg. Fujita, J. Cryst. Growth **196**, 41 (1999).

[6] M. Ogawa, M. Funato, T. Ishido, Sz. Fujita, and Sg. Fujita, Jpn. J. Appl. Phys. **39**, L69 (2000).

[7] M. J. Paisley, Z. Sitar, J. B. Posthill, and R. F. Davis, J. Vac. Sci. Technol. A **7**, 701 (1989).

[8] M. Funato, T. Ishido, Sz. Fujita, and Sg. Fujita, Appl. Phys. Lett. **76**, 330 (2000).

[9] C. Cheng, R. J. Needs, and V. Heine, J. Phys. C **21**, 1049 (1988).

[10] A. F. Wright, J. Appl. Phys. **82**, 5259 (1997).

[11] For the optimization of the growth condition in terms of ZB-GaN, see Refs. 5 and 6.

[12] S. Yamamoto, K. Kaisei, K. Shimogami, M. Funato, Sz. Fujita, and Sg. Fujita (unpublished).

[13] This method was already validated for ZnS and SiC polytypes.

See M. Murayama and T. Nakayama, Jpn. J. Appl. Phys., Suppl. **32**, 32 (1993).

[14] G. Ramírez-Flores, H. Navarro-Contreras, A. Lastras-Martínez, R. C. Powell, and J. E. Greene, Phys. Rev. B **50**, 8433 (1994).

[15] M. Suzuki and T. Uenoyama, Appl. Phys. Lett. **69**, 3378 (1996).

[16] K. Reimann, M. Steube, D. Fröhlich, and S. J. Clarke, J. Cryst. Growth **189/190**, 652 (1998).

[17] L. Eckey, A. Hoffmann, P. Thurian, I. Broser, B. K. Meyer, and K. Hiramatsu, in *Nitride Semiconductors*, edited by F. A. Ponce, S. P. DenBaars, B. K. Meyer, S. Nakamura, and S. Strile, MRS Symposia Proceedings No. 482 (Materials Research Society, Pittsburgh, 1998), p. 555.

[18] M. Murayama and T. Nakayama, Phys. Rev. B **49**, 4710 (1994).

[19] H. P. Maruska and J. J. Tietjen, Appl. Phys. Lett. **15**, 327 (1969).

[20] T. Detchprom, K. Hiramatsu, K. Itoh, and I. Akasaki, Jpn. J. Appl. Phys. **31**, L1454 (1992).